Exp Fluids
DOI 10.1007/s00348-007-0444-6

RESEARCH ARTICLE

Particles for tracing turbulent liquid helium

Gregory P. Bewley · K. R. Sreenivasan · Daniel P. Lathrop

Received: 14 December 2006 / Revised: 30 November 2007 / Accepted: 6 December 2007

Abstract We address the problem of making quantitative measurements of local flow velocities in turbulent liquid helium, using tracer particles. We survey and evaluate presently available particles and previous work to establish the need to develop new particles for the purpose. We present the first practical solution for visualizing fluid motions using a suspension of solid hydrogen particles with diameters of about 2 μm. The hydrogen particles can be used to study flows with Taylor-microscale Reynolds numbers between 85 and 775. The particles can be used equally well with the PIV, LDV, or particle-tracking techniques.

List of symbols

A	Hamaker's constant
d	particle diameter
g	acceleration of gravity
k_B	Boltzmann's constant
L	characteristic size of the large eddies
N	number of particles
n	number of particles per unit volume
T	temperature
U	characteristic velocity of the large eddies
u	local and instantaneous fluid velocity
V_p	total volume of the particles
V_f	total volume of the fluid
V_o	volume of laser sheet that is visible to the camera
v	particle velocity
$\Delta\rho$	density difference between particle and fluid
ε	mean energy dissipation rate
Φ	volume fraction of particles in the fluid
μ	dynamic viscosity of the fluid
ν	kinematic viscosity of the fluid
ρ_f	mass density of the fluid
ρ_p	mass density of the particle

G. P. Bewley
Yale University, New Haven, CT 06520, USA

G. P. Bewley (✉) · D. P. Lathrop
University of Maryland, College Park, MD 20740, USA
e-mail: gregory.bewley@ds.mpg.de

K. R. Sreenivasan
International Centre for Theoretical Physics, 34014 Trieste, Italy

1 Introduction

There is considerable interest in high Reynolds number flows because of their ubiquity in applications. On a basic level, it is only at high Reynolds numbers that statistical properties of turbulence are expected to exhibit universal scaling; see, for example, Monin and Yaglom (1975), Frisch (1995), and Sreenivasan (1999). Defining the turbulence Reynolds number as

$$Re = UL/\nu, \tag{1}$$

where ν is the kinematic viscosity of the fluid, U is the mean or the root-mean-square velocity, and L is the integral length scale, we note that cryogenic helium is attractive for experimental studies because its kinematic viscosity is lower than that of any other known fluid (see, for example, Sreenivasan and Donnelly 2001). This property, along with others such as the large thermal expansion coefficient of cold gaseous helium, has led several research groups to encourage fluid dynamics experiments using helium (Castaing et al. 1992; Smith et al. 1999; Skrbek

et al. 1999; Sreenivasan and Donnelly 2001; Fuzier and Van Sciver 2001; Skrbek 2004; Niemela and Sreenivasan 2006). In this study, we consider liquid helium in its normal fluid phase, because the low viscosity of cryogenic helium enables flows with large Reynolds numbers to be generated on physical scales easily realizable in the laboratory.

Even so, measurements of turbulence in liquid helium are scarce because of the limited number of measurement techniques available. Several research groups have adapted techniques used in common fluids to cryogenic environments, such as particle image velocimetry (PIV) by White et al. (2002) and Zhang and Van Sciver (2005), laser Doppler velocimetry (LDV) by Nakano and Murakami (1992), and hot wires by Castaing et al. (1992). (The promising technique of particle-tracking has only recently been implemented in cryogenic fluids in our laboratory and will be published separately.) Adapting any of these tools to helium poses technical challenges, because the use of cryogenic fluids places great constraints on the spatial resolution of measurement: the advantage of being able to create high Reynolds number helium flows in small apparatus means that the corresponding smallest scales will be that much smaller.

Thus, in developing PIV, LDV, or particle-tracking tools for measuring fluid motions of liquid helium, the critical step is to develop a suitable passive tracer particle. The difficulty lies in the manufacture of such a particle. Below, we discuss the characteristics of suitable and unsuitable particles, review candidate particles and techniques that are available, and present a new method for making small particles. A somewhat parallel effort at Florida State University has recently produced a similar review (Zhang et al. 2004).

2 Difficulties of observing liquid helium flows

2.1 Small length scales

The same property, low viscosity, which makes liquid helium valuable for generating a high Reynolds number flow, also makes the observation of its fluid motions difficult. The statement can be clarified by examining a measure of the smallest scales of motion, η, derived by Kolmogorov (1941),

$$\eta = \nu^{3/4} \Big/ \varepsilon^{1/4}, \tag{2}$$

where $\varepsilon = -m^{-1}\mathrm{d}E/\mathrm{d}t$ is the dissipation rate of the flow's average kinetic energy per unit mass, E/m. By using a Kolmogorov model for the dissipation, ε, which by dimensional arguments is proportional to U^3/L and independent of viscosity at large Reynolds numbers (e.g., Sreenivasan 1984), we see that the small scale shrinks with increasing Re, for fixed L

$$\eta \sim \left(\nu^3 L \big/ U^3\right)^{1/4} = LRe^{-3/4}. \tag{3}$$

To resolve all scales of motion, our measurement probe must correspondingly become smaller. For conditions obtainable by stirring liquid helium, the Kolmogorov scale, η, is typically of the order of a few micrometers.

2.2 Particle suspensions

We desire that the velocity of the particle be close to the local fluid velocity in the absence of the particle. For making velocity measurements of the more common fluids, water and air, the choice of tracer particle is most frequently limited by imaging requirements—the particle must be large enough that it can be imaged with the available illumination and detection equipment. In cryogenic fluids such as liquid helium, there are at least three additional complications.

The low viscosity of the fluid requires that we consider the fidelity with which the particle follows the fluid motions. In addition, the low density of liquid helium, which at its boiling point is one-eighth that of water, compounds the problem of small viscosity. This is so because almost all solid materials are significantly denser than liquid helium, with the notable exception of solid hydrogen, whose density is within 50% of that of liquid helium. Finally, particle aggregation is probably unavoidable in liquid helium. Aggregation is an empirical fact, but we also briefly discuss in the Appendix the mechanism for particle aggregation due to van der Waals forces. In summary, particles in a turbulent flow may be both brought together and pulled apart by motions of the fluid. We consider the balance of these interactions, and find that since the attractive van der Waals force dominates, particles aggregate into ever-larger clusters at a predictable rate. We show below that aggregates are often too large to trace turbulent flows accurately. However, the aggregation rate of a suspension of hydrogen particles generated by our technique is low enough that accurate velocity measurements can be made during a useful window in time.

3 A method to evaluate a tracer particle

Researchers have studied particle dynamics in unsteady flows and evaluated them as possible fluid flow tracers (e.g., Mei 1996). We offer a simple method to evaluate particles, where all the information is contained in a single parameter

as defined below. Following White (2001), we initially measure the fidelity with which a particle follows the fluid flow using two parameters, the Stokes number and the Froude number. The centrality of these parameters follows from an approximation to the equation of motion for the particle, whose full form was proposed by Maxey and Riley (1983).

>Consider a particle whose inertia balances the sum of the buoyancy force and drag proportional to the velocity difference between the particle and the fluid. This simplified description may be valid when the particle-Reynolds number, $Re_p = (u - v)d/v$, is smaller than one, and yields the following equation for the change in momentum of a particle:

$$\tau_p \partial v/\partial t = v_p - (u - v), \tag{4}$$

where u is the local fluid velocity and v is the particle velocity. The particle response time, τ_p, and settling velocity, v_p, are

$$\tau_p = \rho_p d^2/18\mu, \tag{5}$$

and

$$v_p = \Delta\rho d^2 g/18\mu, \tag{6}$$

where d is the particle diameter, ρ_p is the particle density, μ is the dynamic viscosity, $\Delta\rho$ is the difference in density between the particle and the fluid, and g is the acceleration of gravity. These expressions follow directly from the equation of motion using Stokes formula for drag (Batchelor 1967) and the particle density times its volume for its inertia. We then introduce characteristic velocity and time scales of the flow, u_f and τ_f respectively, and solve for the difference in velocity between the fluid and the particle,

$$(u - v)/u_f = Fr - St\partial v/\partial t(\tau_f/u_f). \tag{7}$$

Here, $St = \tau_p/\tau_f$ and $Fr = v_p/u_f$, where St is the Stokes number, measuring the importance of the particle inertia, and Fr is the Froude number, measuring the importance of the particle settling velocity. We infer from (7) that the fractional error in measurement of the fluid velocity, $(u - v)/u_f$, is roughly the value of the Stokes or Froude number, whichever is larger.

We evaluate the Stokes and Froude numbers for candidate particles by choosing the fluid time and velocity scales to be the Kolmogorov scales in the flow

$$\tau_f = (v/\varepsilon)^{1/2}, \tag{8}$$

and

$$u_f = (v\varepsilon)^{1/4}, \tag{9}$$

which measure the fine scales of flow (see Frisch 1995). If the particles are able to respond to these motions, they will also trace the range of motions present in a turbulent flow.

In liquid helium, almost any choice of particle yields Stokes and Froude numbers near unity in easily obtainable flow conditions. Assume that there are values St_{max} and Fr_{max}, above which deviation of the motion of a particle from the motion of the fluid becomes too large. The results of Wells and Stock (1983), Mei et al. (1990), Reeks (1977), and Voth et al. (2002) suggest that observing the motions of particles with Stokes and Froude numbers in the range 0.3–0.5 result in measurements of kinetic energy and integral length scale that are within 5–10% of the fluid's actual large scale properties. [Here, we have renormalized the results we refer to according to our own definitions for the Stokes and Froude numbers, as in Bewley (2006).] To obtain negligible errors in such measurements due to particle dynamics, we choose to target values that are an order of magnitude smaller, namely

$$St_{max},\ Fr_{max} = 0.05. \tag{10}$$

In conjunction with (7), this limit states that the typical difference in velocity between a particle and the surrounding fluid is about 5%. This objective, in turn, imposes constraints on the range of Reynolds numbers observable using a particular particle.

To see this, we recast the Stokes and Froude numbers in terms of the Reynolds number. We then find bounds in terms of the Reynolds number for which a particular particle can be considered to represent a fluid parcel. Using Kolmogorov's relation for homogeneous and isotropic turbulence, $\varepsilon \cong U^3/L$, we regroup the definitions of St and Fr, and find that

$$18St_{max} > (\rho_p/\rho_f)(d/L)^2 Re^{3/2} \tag{11}$$

and

$$18Fr_{max} > (\Delta\rho/\rho_f)(d^2 gL/v^2)Re^{-3/4}. \tag{12}$$

We have chosen, in our introduction of Re, to remove the explicit appearance of the characteristic velocity, U. We then write our expressions equivalently in terms of limits on the Reynolds number,

$$Re_{max}^{3/2} = 18St_{max}(L/d)^2(\rho_f/\rho_p) \tag{13}$$

$$Re_{min}^{3/4} = (18Fr_{max})^{-1}(d^2 gL/v^2)(\Delta\rho/\rho_f). \tag{14}$$

The minimum Reynolds number stems from the need to maintain turbulent intensity so that the settling velocity of the particle does not dominate its motion. The maximum Reynolds number stems from the resistance of particle inertia to large accelerations in an intensely turbulent flow. Note that a neutrally buoyant particle can be used at arbitrarily low Reynolds numbers. In this case, Re_{max} alone is the limiting parameter.

In order for there to exist a range of Reynolds numbers for which the particle is useful according to these criteria, the ratio

$$B = \frac{Re_{\max}}{Re_{\min}} \approx \left[\frac{\rho_f^3}{\rho_p \Delta \rho^2}\right]^{\frac{2}{3}} \left[\frac{\nu^2}{g d^3}\right]^{\frac{4}{3}} \quad (15)$$

must be larger than one. We have used the fact that $18St_{\max}$ and $18Fr_{\max}$ are both approximately equal to one, according to (10). In contrast to the parameters St and Fr, which depend on time and the initial conditions in an evolving flow, the ratio, B, does not depend on U or L, and is independent of the flow. The ratio depends only on the physical properties of the fluid and particle and is particularly sensitive to the particle size.

In the above analysis, we estimate and predict how to minimize the magnitude of the deviations of the particle motion from the fluid motion. Including additional terms such as those given by Maxey and Riley (1983) in the particle equation of motion, (4), results in additional parameters, but minimizing the Stokes and Froude numbers alone probably minimizes all contributions to these deviations. For example, inclusion of the 'added mass' term results in a parameter that is equal to $1/2St$ when the particle density and fluid density are comparable. To refine the result we present, further work to understand the detailed motions of particles is required.

4 Evaluation of available seeding techniques

4.1 Hollow glass spheres

At least two companies, PQCorp and 3M, manufacture hollow shells made of glass. The companies specify that the diameters of such particles range from about 10 μm to several hundred microns in a typical sample, and that the density of the particles are close to that of liquid helium, between 0.14 and 0.19 g/cc. According to our analysis, we require a particle smaller than 5 μm in diameter, and with a density that is less than or equal to 0.14 g/cc.

Through a microscope, one can see particles that range in size from 1 to 30 μm. However, a simple test reveals that even the smallest hollow particles are close to 10 μm in diameter. We inject particles at the bottom of a cylinder filled with methanol, and collect those that rise to the surface after various periods of time from the time of injection. The smallest particles that rise are in the diameter range between 9 and 16 μm. At the bottom of the column lie the smaller particles, between 1 and 15 μm in diameter. These particles are either solid glass or incomplete shells. As revealed in Table 1, the small difference from the required size is critical.

Table 1 The properties of candidate tracer particles

Particle material	Diameter (μm)	Density (g/cc)	B
Hollow glass	9	0.14	0.5
Polystyrene particle aggregate	4	1.06	0.02
Hydrogen	2	0.088	86

Listed are the B numbers, defined by (15), for a variety of particles in liquid helium near its boiling point. Only the hydrogen particles satisfy our condition that $B > 1$, and thereby can be used to trace accurately the motions of turbulent liquid helium.

4.2 Solid beads

Several manufacturers produce solid spherical particles in a wide range of tightly controlled diameters. Experimentalists seeking tracers for water often use particles of this type. Particle densities range from just over that of water, 1.06 g/cc for polystyrene microspheres, to several grams per cubic centimeter for solid glass microspheres. For a typical turbulent flow, we seek a solid particle that is smaller than 1 μm. Zhang and Van Sciver (2005) used such polystyrene particles to observe thermally driven flows in liquid helium. We considered making velocity measurements using particles of this type, made from a variety of materials.

We observed that solid particles form clusters in a cryogenic fluid. We tried several techniques for injecting and agitating them, as well as using particles made of various materials. The particle images always appear with a wide range of intensities typical of a polydisperse distribution (see Fig. 1, left), rather than the uniform appearance of similar monodisperse particles suspended in water (see Fig. 1, right). As suggested in our brief discussion of the physics of aggregation in the Appendix, the particles probably bind to each other during or before injection, when they are necessarily highly concentrated.

We estimate based on the intensity of light scattered by the particle clusters that the aggregates are roughly at least three particle diameters across. Such a technique for measuring particle size, though inaccurate, does show that the particle clumps must be larger than individual particles. As further supporting evidence for the existence of clusters, we note that Zhang and Van Sciver (2005) report the settling velocity of 1.7 μm polystyrene particles in liquid helium as 6 mm/s, though the settling velocity for such particles is about 1.1 mm/s according to (6) under the reported conditions. The reported settling velocity is closer to the settling velocity of a 4 μm particle, which is probably a cluster of smaller spheres. As shown in Sect. 6.7, a clump is probably not adequate for making accurate measurements of flow velocities.

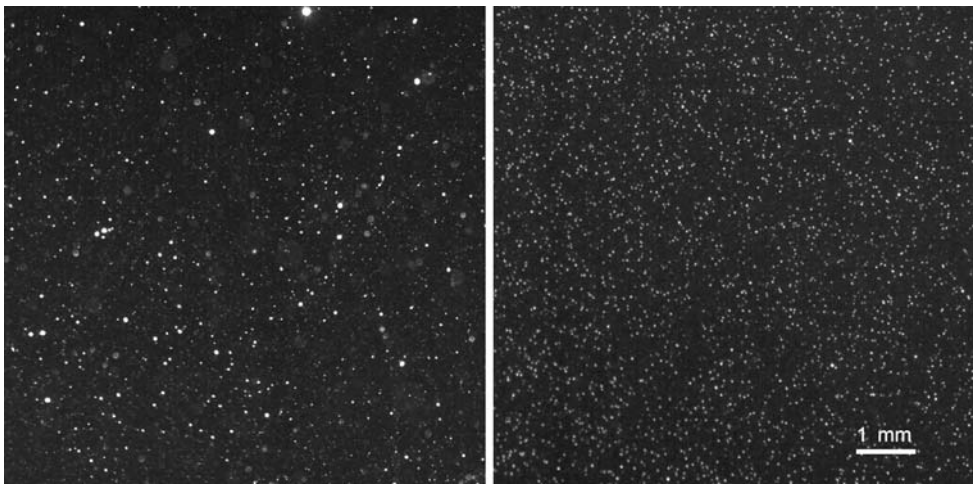

Fig. 1 On the left are clumps of 2 μm polystyrene particles in liquid helium. On the right are identical particles in water, using a surfactant to disperse them

4.3 Other types of particles

We have also considered the suitability of other commercially available particles and powders. These include silica aerogels, polymer microballoons, carbonized microballoons, Teflon powders, porous ceramic powders, frozen electrosprays, and pollen. We determined that they could not be useful, usually because of particle diameter, although we do not rule out the possibility that any of these products could be made to work with greater effort. We also attempted to freeze a fine mist of hydrogen droplets by pushing liquid hydrogen through a 100 μm orifice at high pressure into liquid helium. This method failed, because the particles we generated were several tens of microns in diameter or larger.

4.4 Review of previous work to make frozen particles

The effort to seed liquid helium with tracer particles dates back to 50 years when Chopra and Brown (1957) injected a mixture of hydrogen and deuterium gas into liquid helium through a heated nozzle. They were able to make millimeter size solid particles, and noted that the particles tended to stick to each other and to the walls of the container. Subsequent efforts refined the procedure and reduced the size of the resultant particles. For example, researchers injected hydrogen gas into a cryostat through a large nozzle of order 1 mm in diameter. Chung and Critchlow (1965) report particles with sizes of several hundred microns and Kitchens et al. (1965) report 20–100 μm particles, both the groups working in superfluid helium. More recently, Murakami and Ichikawa (1989) and Nakano and Murakami (1992) report creating micron-sized hydrogen particles in superfluid helium, although they include no evidence to support their claim on the particle diameter. Celik et al. (1999) have undertaken an effort to make a hydrogen atomizer to generate smaller particles, though they do not estimate the resulting particle's size. Celik and van Sciver (2002) report the generation of 10 μm neon particles using a similar apparatus. Newly published work describing hydrogen particles in superfluid helium is that of Xu and Van Sciver (2006) and Takakoshi and Murakami (2006).

Several groups, including our own, independently made a key advance, which is the dilution, at room temperature, of hydrogen with large amounts of helium gas. Boltnev et al. (2002) pass this dilute mixture through a nozzle above the liquid helium bath, forming a jet that impinged on the free surface, and report the possible existence of submicron particles. Their goal, however, is quite different from ours; they had no interest in tracing fluid motions.

5 Apparatus

We use a liquid nitrogen-jacketed cryostat with optical access to the liquid helium provided by four windows. The cryostat is modified from a standard Janis product. To the bottom of a 6-liter helium reservoir is fixed a custom sample cell designed for studying grid-generated turbulence. It is a 25-cm long channel with a 5 cm by 5 cm square cross section. This channel communicates with the main liquid reservoir through a 1.5-mm tube, which allows it to remain filled with liquid. Windows on each face of the channel, 10 cm from the bottom of the channel, have an optical aperture of 2.5 cm. Three tubes with 9 mm inner diameter provide access to the experimental chamber.

An argon ion laser illuminates suspended particles with up to 6 W of light. Cylindrical lenses form the laser beam into a thin sheet with nearly uniform intensity across its height of 1.5 cm. The thickness of the beam is about 100 μm according to the theory of Gaussian optics. A CMOS camera with 1 GB of onboard memory and a

square, one megapixel sensor is aimed at the illuminating light sheet. Pixels are 16 μm across, and we use a 105-mm Nikon macrolens with a magnification of one. The camera observes an area of dimension 1.6 × 1.6 cm, and collects and stores 1,012 image frames at up to 1,000 frames/s.

6 Results and discussion

6.1 The injector

We produce hydrogen particles by diluting hydrogen gas with helium at room temperature, and passing the mixture through an injector directly into the liquid. The injector is illustrated in Fig. 2. It is a straight tube extending from the lab to the liquid helium-filled channel through one of the cryostat's access ports. The inner diameter of the injector is 3 mm. A concentric tube of larger diameter sheaths the length of the inner tube, and the space between the tubes is sealed. Atmospheric gases in this annular space are thought to condense when the injector is cold, forming an insulating vacuum jacket.

A mixture of hydrogen and helium gas is prepared in a bottle at room temperature. Typically, the bottle is flushed with hydrogen gas, allowed to vent to atmospheric pressure, and helium gas is added to a pressure yielding the desired mixture ratio.

The mixture is supplied to the injector with a small amount of pressure, about 30 kPa, which is further reduced through a needle valve. We open a valve until the formation of particles is observed through the cryostat windows. Valve position is maintained at this setting for several seconds, until the liquid helium is adequately seeded with particles.

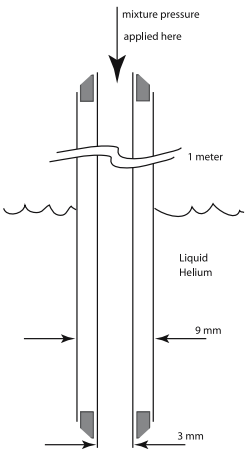

Fig. 2 The schematic shows the design of our diluted hydrogen injector. Hydrogen gas diluted with helium is introduced at the top and enters the cryostat through the inner of two concentric stainless steel tubes. The mixture cools on passage through the injector and exits below the free surface of liquid helium

6.2 Hydrogen concentration

We show an example of particles produced using the hydrogen mixture injector in Fig. 3. We find that the number of aggregates larger than about 30 μm rises when using mixtures more concentrated than $1H_2$:5He by volume. In addition, the characteristic particle size shrinks as the hydrogen is diluted. For mixtures more dilute than $1H_2$:500He, we do not resolve individual particles but observe diffuse light scattered from a hydrogen fog. The liquid, prior to injection, does not visibly scatter light at the intensities we use ($\sim$100 W/cm^2). We often use a mixture ratio of $1H_2$:50He as a compromise between particle size and number.

6.3 Particle size

The injector introduces 25 cm^3/s of gas, as measured at standard temperature and pressure. For an injection with a duration of 5 s using a mixture with a dilution ratio of $1H_2$:10He, 0.013 cm^3 of solid hydrogen is introduced to the cryostat. If all this hydrogen is deposited in the particle

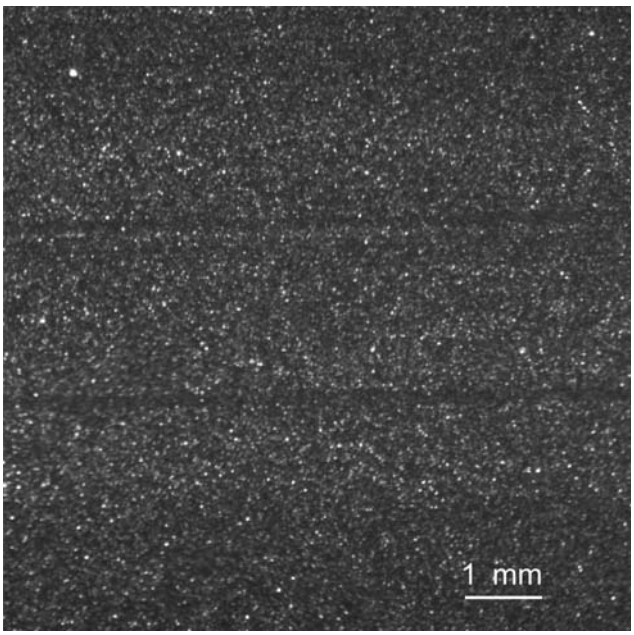

Fig. 3 We show a 512 × 512 pixel image of hydrogen particles taken about 1 min after being generated in liquid helium at 4.2 K using hydrogen gas diluted with helium gas in a 1:10 ratio. The particle distribution appears to be polydisperse. The vertical gradients in intensity are due to nonuniformities in the illuminating laser sheet

suspension, the volume of hydrogen particles, V_p, relative to volume of the liquid helium in the cryostat, V_f = 2,000 cm^3, is

$$\Phi = V_p/V_f \approx 6 \times 10^{-6} \pm 30\%. \quad (16)$$

This volume fraction is small enough that the particles have a negligible effect on the viscosity of the fluid (Batchelor 1967).

We use the particle volume fraction to estimate the characteristic size of the particles by counting particle images. The number of particles, N_p, is related to the volume fraction by

$$\pi N_p d_c^3/6 = V_o \Phi, \quad (17)$$

for particles of characteristic diameter d_c in the image volume, V_o. For a 5 s injection of $1H_2$:10He gas, we use a particle-counting algorithm to find about 4×10^4 particles per image, although the count varies by up to 25% depending on the parameters used to define a particle. We estimate the image volume using the image dimensions and light sheet thickness given in Sect. 5. Although the particles may have a wide distribution of sizes, and despite large uncertainties in the measurements, we estimate the characteristic particle diameter,

$$d_c = 1.8 \ \mu\text{m} \pm 30\%, \quad (18)$$

with surprising accuracy, since the measurements are proportional to the cube of the particle size. This diameter is much smaller than the resolution of our camera, and the sizes of particle images are determined by diffraction and by blooming on the camera sensor, whose extent depends on the intensity of the light scattered by each particle. In addition, we assume that all the hydrogen we inject forms visible particles. If some of the injected hydrogen forms particles that scatter too little light to be detectable, or particles that are so large that they rise immediately out of view, then we overestimate the size of the visible particles. It follows that the particles would only be better tracers than we claim here.

6.4 Model of injector function

Here we discuss a possible mechanism by which the particles are formed during injection. At atmospheric pressure, hydrogen liquefies at 22 K and solidifies at 14 K, well above the working temperatures for liquid helium. The mixture of hydrogen and helium gas cools as it descends through the injector into the cryostat, and the hydrogen precipitates, which can occur in binary mixtures by homogeneous nucleation (Wegener and Sreenivasan 1981). We expect a wide distribution of particle sizes, since the formation of nuclei and the growth and aggregation of existing nuclei can occur simultaneously. If the rate of aggregation of nuclei can be described as in the Appendix, we expect that the characteristic size of particles depends inversely on the hydrogen concentration. The process of precipitation continues until the mixture reaches thermal equilibrium with the liquid helium in the bath, where the particles are dispersed into the liquid.

6.5 Practical considerations

An advantage of hydrogen particles is that they form as a dispersed suspension. Premanufactured solid particles must be stored and introduced as a concentrated solution with the attendant problem of aggregation. In addition, since the settling velocity of a particle is proportional to the square of its size (see Sect. 3), buoyancy rapidly moves large hydrogen particles aggregates to the free surface of the liquid helium, effectively removing them from the system. Aggregation and buoyancy act to clean the system of particles, and we can periodically generate new small particles. The process of creating hydrogen particles is simple and swift, requiring little of the preparation required for other types of particles (see White 2001; Zhang et al. 2004).

Hydrogen particles accumulate on the windows, as do the other particles we tested. We remove hydrogen particles by warming the system enough to vaporize them, whereas other types of particles may require the system to be disassembled. A problem that affects all particle types in liquid helium is that the particles have many different sizes because of aggregation. A solution that yielded monodisperse particles would be beneficial from the point of view of imaging requirements. Finally, precautions must be taken since hydrogen is flammable.

6.6 A note on the injection of particles into superfluid helium

At temperatures lower than 2.17 K, liquid helium is a superfluid, and particles can also be used as tracers of superfluid flows. At these temperatures, particle behavior is complicated by interactions with both the normal viscous fluid and the inviscid superfluid (Poole et al. 2005) and cannot be evaluated according to the analysis we present in the Sect. 3. Many experimenters mentioned in Sect. 4.4 focused on producing hydrogen particles in the superfluid. We found that our method fails when injecting particles directly into the superfluid, because the hydrogen forms aggregates larger than 10 μm in size, rather than the smaller particles we described above. The way we suspend

small particles in the superfluid is to form the particles at higher temperatures, in normal helium, and then to cool the fluid and particles together to the desired superfluid state (Bewley et al. 2006).

6.7 Comparison of particles

In Table 1, we summarize the utility of the particles surveyed in this study. As described in Sect. 3, a B number greater than one indicates that there exists a range of Reynolds numbers for which the particles will trace the motions of homogeneous and isotropic turbulence in liquid helium with adequate fidelity. For comparison, the B numbers for any of these particles in water is greater than 10^3. We note that for individual 0.8 μm polystyrene particles, $B = 8.5$, but as discussed in the Appendix, it is unlikely that they can be suspended as individual particles, since they have a strong tendency to aggregate into larger clumps. As shown in the table, these clumps are not suitable tracers. In addition, $B = 13$ for 4 μm hollow glass spheres, but we do not know of any that are manufactured. Finally, it is possible to generate nearly neutrally buoyant particles by mixing hydrogen with deuterium. These particles can be used at arbitrarily low Reynolds numbers and the B number is inapplicable. However, the high-Reynolds number behavior of the particle is similar to that of a simple hydrogen particle, which we discuss below.

To determine the suitable range of Reynolds numbers for the hydrogen particles, one must specify some detail of the flow the particle is required to trace. The integral length scale, L, of flows in a bench-top cryostat is typically about 0.5 cm. For a 2 μm hydrogen particle in liquid helium, and using the relation $Re_\lambda \approx (15Re)^{1/2}$, the acceptable Taylor scale-based Reynolds numbers, Re_λ, range from 85 to 775, according to (13) and (14).

As a practical example, we use the hydrogen particles to observe turbulence in rotating liquid helium. As described in Bewley et al. (2007), we use hydrogen particles and the PIV technique (Adrian and Yao 1983) to observe grid-generated turbulence with a Taylor-based Reynolds number of about 260.

7 Conclusion

We have shown previously that available particles are inadequate for making precise measurements of velocities in turbulent liquid helium. We present a simple way of making hydrogen particles that are likely to be small enough to make such measurements. We estimate that the particles are typically about 2 μm in diameter. We also find that particles have a tendency to clump that may be insurmountable in cryogenic fluids, and that this problem is most severe at the moment of particle injection. Finally, we establish well-defined limits in terms of fluid and flow properties for which particles of particular characteristics can be used. These hydrogen particles may be appropriate for studying flows in liquid helium over a wide range of Reynolds numbers. In closing, we note that these particles could also be used to study flows in cryogenic gaseous helium.

Acknowledgments The National Science Foundation of the USA and NASA supported this work. We wish to thank Chris White for guidance, and Russ Donnelly, Joe Niemela, Steve Predko, and Joe Vinen for the cryostat.

8 Appendix

We have observed the aggregation of several types of particles in liquid helium, and we argue here that aggregation may be unavoidable in this fluid. The forces that draw particles together are the same as the ones that binds the molecules of the particle together to form a solid, known as the van der Waals forces. This force overwhelms Brownian motion for particles that come close to each other, as we see if we consider the attractive potential, U_D, between two spheres with center to center separation r and with radius a,

$$U_D = \frac{-A}{6}\left[\frac{2a^2}{r^2-4a^2} + \frac{2a^2}{r^2} + \ln\left(\frac{r^2-4a^2}{r^2}\right)\right], \tag{19}$$

which is a function of Hamaker's constant, A (Vold and Vold 1983). Thermal energy is measured by $E_T = k_B T \approx 6 \times 10^{-23}$ J, where k_B is Boltzmann's constant, and T is the temperature, and the value is given for $T = 4.2$ K. The value of r for which $U_D = E_T$ is approximately $r_c = 4a$, using Hamaker's constant for polystyrene, $A = 8 \times 10^{-20}$ J, although the Hamaker constant for most materials is of the same order. Note that an exception is liquid helium, and since Hamaker's constant for liquid helium is much smaller (Paalanen and Iye 1985), we do not need to account for it as the intervening fluid (Hiemenz and Rajagopalan 1997). Within 2 diameters, the van der Waals potential rises sharply, and it is therefore unlikely that thermal fluctuations will separate particles under its influence.

Most methods to prevent particles from coalescing under the influence of the van der Waals potential are inapplicable in liquid helium. The first, steric stabilization, can be accomplished by manufacturing particles with a surface coating or by adding a surfactant. This solution depends on the flexibility of polymer molecules (Vold and Vold 1983), and in liquid helium the mechanism fails because its temperature is below the glass transition temperature of all polymers. The second method uses

electrostatic repulsion. To exploit this force, one can manufacture particles with polar groups on the particle surface, or cause the particles to accumulate free ions. The dissociation of an ion that allows the formation of a polar group requires a polar solvent, such as water. Since helium is nonpolar, this solution is inapplicable. However, adding an electrostatic charge to particles was implemented successfully in liquid nitrogen (Huber and Wirth 2003), and the method is potentially useful for dispersing particles in liquid helium.

Since the van der Waals potential given in (19) diverges to infinity as the separation between particles becomes smaller, the theory predicts that particles are inseparable once they come into contact. Without a method to prevent particles from coalescing, one must know the mechanical properties of the particles, or perform experiments to measure the strength of the bond between particles under the relevant conditions, to understand how to break particle aggregates apart. We are not aware of such work having been done.

It is known that the shear inherent to turbulence both causes particle collisions (Saffman and Turner 1956) and breaks apart particle aggregates (Sonntag and Russel 1986). Based on the above discussions, we assume that turbulence cannot break aggregates at the intensity we are able to generate it. If particles are inseparable, we estimate the rate of aggregate growth as follows. Saffman and Turner (1956) give a solution for the particle number density as a function of time under the assumption that the collision frequency is independent of particle size:

$$n = n_0/(1 + \alpha n_0 t). \tag{20}$$

Here, n is the total number of particles per unit volume, with initial value n_0, and α is the collision frequency, where $\alpha = 1.30a^3 vRe^{3/2}/L^2$. The time for the particle number to halve is

$$\tau_{1/2} \approx \pi L^2 \Big/ \left(\Phi v Re^{3/2}\right), \tag{21}$$

where Φ is the volume fraction of particles relative to the fluid, and is equal to $4\pi a^3 n_0/3$.

For typical conditions in turbulent liquid helium, the time constant given by (21) is about 5 min. This indicates that if particles of the desired initial size were dispersed, there exists a useful period of time during which they are fluid tracers. However, $\tau_{1/2}$ is inversely proportional to the particle volume fraction. If the particles must be injected into the fluid as a concentrated solution, and this process is necessarily turbulent, then at the time of injection and near the injector the volume fraction of particles is larger than in the fully dispersed solution. For particles at an initial volume fraction of 0.1 injected at 10 cm/s through a 3-mm injector, $\tau_{1/2}$ is reduced to about 0.01 s. This leaves little time for the particles to leave the injector before they irreversibly clump into larger particles.

References

Adrian RJ, Yao CS (1983) Development of pulsed laser velocimetry for measurement of fluid flow. In: Patterson G, Zakin JL (eds) Proceedings, eighth biennial symposium on turbulence. University of Missouri, Rolla

Batchelor GK (1967) An introduction to fluid dynamics. Cambridge University Press, Cambridge

Bewley GP (2006) Using hydrogen particles to observe rotating and quantized flows in liquid helium. PhD Thesis, Yale University

Bewley GP, Lathrop DP, Maas LRM, Sreenivasan KR (2007) Inertial waves in rotating grid turbulence. Phys Fluids 19:071701

Bewley GP, Lathrop DP, Sreenivasan KR (2006) Visualizing quantized vortices. Nature 441:588

Boltnev RE, Frossati G, Gordon EB, Krushinskaya IN, Popov EA, Usenko A (2002) Embedding impurities into liquid helium. J Low Temp Phys 127:245–258

Castaing B, Chabaud B, Hebral B (1992) Hot wire anemometer operating at cryogenic temperatures. Rev Sci Instrum 63:2442–2446

Celik D, Smith MR, Van Sciver SW (1999) A particle seeding apparatus for cryogenic visualization. Adv Cryog Eng 45:1175–1180

Celik D, Van Sciver SW (2002) Tracer particle generation in superfluid helium through cryogenic liquid injection for particle image velocimetry (PIV) applications. Exp Therm Fluid Sci 26:971–975

Chopra KL, Brown JB (1957) Suspension of particles in liquid helium. Phys Rev 108:157

Chung DY, Critchlow PR (1965) Motion of suspended particles in turbulent superflow of liquid helium II. Phys Rev Lett 14:892–894

Frisch U (1995) Turbulence: the legacy of A.N. Kolmogorov. Cambridge University Press, Cambridge

Fuzier S, Van Sciver SW (2001) Steady-state pressure drop and heat transfer in He II forced flow at high Reynolds number. Cryogenics 41:453–458

Hiemenz PC, Rajagopalan R (1997) Principles of colloid and surface chemistry. Marcel Dekker, New York

Huber G, Wirth KE (2003) Electrostatically supported surface coating of solid particles in liquid nitrogen for use in dry-powder inhalers. Powder Tech 134:181–192

Kitchens TA, Steyert WA, Taylor RD (1965) Flow visualization in He II: direct observation of Helmholtz flow. Phys Rev Lett 14:942–945

Kolmogorov AN (1941) The local structure of turbulence in incompressible viscous fluid for very large Reynolds numbers. Proc R Soc Lond A Math Phys Sci 434:9–13 (1991)

Maxey MR, Riley JJ (1983) Equation of motion for a small rigid sphere in a nonuniform flow. Phys Fluids 26:883–889

Mei MR (1996) Velocity fidelity of flow tracer particles. Exp Fluids 22:1–13

Mei MR, Adrian RJ, Hanratty TJ (1990) Particle dispersion in isotropic turbulence under stokes-drag and basset force with gravitational settling. J Fluid Mech 225:481–495

Monin AS, Yaglom AM (1975) Statistical fluid mechanics, vol 2. MIT Press, Cambridge

Murakami M, Ichikawa N (1989) Flow visualization study of thermal counterflow jet in He II. Cryogenics 29:438–443

Nakano A, Murakami M (1992) Measurement of second sound Helmholtz oscillation in He II using laser Doppler velocimeter. Adv Cryog Eng 37A:97–103

Niemela JJ, Sreenivasan KR (2006) The use of cryogenic helium for classical turbulence: promises and hurdles. J Low Temp Phys 143:163–212

Palaanen MA, Iye Y (1985) Electron mobility on thin He films. Phys Rev Lett 55:1761–1764

Poole DR, Barenghi CF, Sergeev YA, Vinen WF (2005) Motion of tracer particles in He II. Phys Rev B 71:064514

Reeks MW (1977) On the dispersion of small particles suspended in an isotropic turbulent fluid. J Fluid Mech 83:529–546

Saffman PG, Turner JS (1956) On the collision of drops in turbulent clouds. J Fluid Mech 1:16–30

Skrbek L (2004) Turbulence in cryogenic Helium. Physica C 404:354–362

Skrbek L, Niemela JJ, Donnelly RJ (1999) Turbulent flows at cryogenic temperatures: a new frontier. J Phys Condens Matter 11:7761–7781

Smith MR, Hilton DK, Van Sciver SW (1999) Observed drag crisis on a sphere in flowing He I and He II. Phys Fluids 11:751–753

Sonntag RC, Russel WB (1986) Structure and breakup of flocs subjected to fluid stresses I. Shear experiments. J Colloid Interface Sci 13:399–413

Sreenivasan KR (1984) On the scaling of the turbulence energy dissipation rate. Phys Fluids 27:1048–1051

Sreenivasan KR (1999) Fluid turbulence. Rev Mod Phys 71:S383–S395

Sreenivasan KR, Donnelly RJ (2001) Role of cryogenic helium in classical fluid dynamics: basic research and model testing. Adv Appl Mech 37:239–276

Takakoshi T, Murakami M (2006) Application of PIV technology to superfluid He II thermal counterflow jet. Proc ICEC 21

Voth GA, La Porta A, Crawford AM, Alexander J, Bodenschatz E (2002) Measurement of particle accelerations in fully developed turbulence. J Fluid Mech 469:121–160

Vold RD, Vold MJ (1983) Colloid and interface chemistry. Addison Wesley, Reading, MA

Wegener PP, Sreenivasan KR (1981) The effect of cooling rate on binary nucleation. Appl Sci Res 37:183–194

Wells MR, Stock DE (1983) The effects of crossing trajectories on the dispersion of particles in a turbulent flow. J Fluid Mech 136:31–62

White CM (2001) High Reynolds number turbulence in a small apparatus. PhD Thesis, Yale University

White CM, Karpetis AN, Sreenivasan KR (2002) High-Reynolds-number turbulence in small apparatus: grid turbulence in cryogenic liquids. J Fluid Mech 452:189–197

Xu T, Van Sciver SW (2006) Solid H2/D2 particle seeding and injection system for PIV measurement in He II. Adv Cryog Eng 51B:1685

Zhang T, Celik D, Van Sciver SW (2004) Tracer particles for application to PIV studies of liquid helium. J Low Temp Phys 134:985–1000

Zhang T, Van Sciver SW (2005) The motion of micron-sized particles in He II counterflow as observed by the PIV technique. J Low Temp Phys 138:865–870